Strain Rate Self-Sensing for a Cantilevered Piezoelectric Beam

Yoonsu Nam*
Department of Mechanical Engineering, Kangwon National University, 192-1 Hyoja 2 dong, Chunchon city, Kangwon-do 200-701, Korea
Minoru Sasaki
Department of Mechanical and Systems Engineering, Faculty of Engineering, Gifu University, 1-1 Yanagido, Gifu 501-1193, Japan

This paper deals with the analytical modeling, and the experimental verification of the strain rate self-sensing method using a hybrid adaptive filter for a cantilevered piezoelectric beam. The piezoelectric beam consists of two laminated lead zirconium titanates (PZT) on a metal shim. A mathematical model of the beam dynamics is derived by Hamilton's principle and the accuracy of the modeling is verified through the comparison with experimental results. For the strain rate estimation of the cantilevered piezoelectric beam, a self-sensing mechanism using a hybrid adaptive filter is considered. The discrete parts of this mechanism are realized by the DS1103 DSP board manufactured by dSPACE™. The efficacy of this method is investigated through the comparison of experimental results with the predictions from the derived analytical model.

Key Words: Piezoelectric Material, Adaptive Filter, Strain Rate Self-Sensing, Hamilton's Principle

Nomenclature

A : Area of electrode
b : Width of piezoelectric beam
C_P : Equivalent capacitance of piezoelectric material
D_3 : Electric charge displacement (charge per unit area)
d_{31} : Piezoelectric material constant
e_{31} : Piezoelectric material constant
E_3 : Electric potential supplied in 3 - axis
E_P^{11} : Young's modulus of piezoelectric material
E_S : Young's modulus of center shim material
E_C : Young's modulus of coating material
h_P : Thickness of piezoelectric material
h_S : Thickness of center shim material
h_C : Thickness of coating material

* Corresponding Author,
E-mail : nys@cc.kangwon.ac.kr
TEL : +82-33-250-6376; **FAX** : +82-33-257-4190
Department of Mechanical Engineering, Kangwon National University, 192-1 Hyoja 2 dong, Chunchon city, Kangwon-do, 200-701, Korea. (Manuscript **Received** April 9, 2001; **Revised** December 10, 2001)

i_{tot} : Total current applied on the piezoelectric material
i_{elec} : Feedthrough current on the piezoelectric material
i_{mech} : Current used for mechanical works
L : Length of piezoelectric beam
m_S : Mass per unit length for shim material
m_P : Mass per unit length for piezoelectric material
m_C : Mass per unit length for coating material
n : Total number of modes in assumed mode expansion
q_{tot} : Total charge applied on the piezoelectric material
q_{mech} : Equivalent charge due to the developed mechanical strain
$r_i(t)$: i-th generalized coordinate
v : Supplied voltage on the electrode
ε_1 : Mechanical strain in 1 - axis
$\in_{33}^S$: Permittivity of piezoelectric material at constant strain
$\phi_i(x)$: i-th mode shape function

ρ_S : Density of shim material
ρ_P : Density of piezoelectric material
ρ_C : Density of coating material

1. Introduction

Due to its advantages in smaller size and weight, and higher bandwidth capabilities as compared to the other devices, the piezoelectric materials have been used extensively as sensors or actuators. The piezoelectric materials can act as a transducer, generating a voltage difference between the two electrodes in response to an imposed force, thus sensing dynamic acceleration, pressure, etc. (Doebelin, 1990). Conversely, the response of piezoelectric materials to the applied voltages allows them to be used as actuators in a wide variety of applications ranging from the vibration to the noise suppression problems (Dimitriadis et al., 1991 ; Clark and Fuller, 1992 ; Evans et al., 1999 ; Ko, 1996 ; Okugawa and Sasaki, 1997 ; Oh et al., 1998). However, the combined actuation and sensing mechanisms (i.e. the self-sensing capability) for the piezoelectric materials are possible and becoming very important for the intelligent mechanical structures. By implanting the piezoelectric materials functioning both as actuators and sensors in the composite materials, the intelligent structures can be made, which change their mechanical properties adaptable for the various operational environments, or which have self-monitoring capabilities of the mechanical structure's malfunction (Crawley and Luis, 1987 ; Ishihara and Arai, 1996).

The idea of self-sensing actuators was concurrently proposed by Dosch et al.(1992) and Anderson et al.(1992). By applying the identical voltages to a piezoelectric actuator and an equivalent capacitor, and comparing the currents from both, the strain rates of the mechanical structure can be estimated. This method, however, turns out to be impractical due to the changes of the piezoelectric capacitance with the operational conditions (Johns et al., 1994 ; Janocha et al, 1994). Clark and et. al. proposed a strain rate self-sensing mechanism using the least-mean-square (LMS) algorithm to resolve the problems of the previous method (Cole and Clark, 1994). They also proposed a hybrid adaptive filter mechanism using the steepest descent algorithm to estimate the strain rate of piezoelectric structure (Vipperman and Clark, 1998). A continuous-time adaptive filter for estimating the strain rate was introduced by Fannin and Saunders (1997).

This paper deals with the analytical modeling and the experimental verification of the strain rate self-sensing method using a hybrid adaptive filter for a cantilevered piezoelectric beam. The piezoelectric beam consists of two laminated lead zirconium titanates (PZT) on a metal shim. Section 2 contains the introduction and working principles of the various self-sensing methods. In Sec. 3, the mathematical model of the cantilevered piezoelectric beam dynamics is derived by Hamilton's principle and the accuracy of the modeling is verified through the comparison with experimental results. Section 4 includes the experimental results from the strain rate self-sensing system. For the strain rate estimation of the cantilevered piezoelectric beam, a self-sensing mechanism using a hybrid adaptive filter is considered. The discrete parts of this mechanism are realized by the DS1103 DSP board manufactured by dSpaceTM. The efficacy of this method is investigated through the comparison of experimental results with those from the analytical method. The effect of convergence factor in the adaptive filter is also experimentally investigated. Finally, the conclusion of this paper and future research areas are summarized in Sec. 5.

2. Methods of Strain Rate Self-Sensing

Basically, the piezoelectric material is an energy transformer, which converts the electrical energy to the mechanical energy, and vice versa. When it is used for an actuation device, only a portion of the supplied electric energy is converted to the useful mechanical energy. The rest is fed through the piezoelectric material, and eventually dissipated as heat in the electric circuits. Figure 1

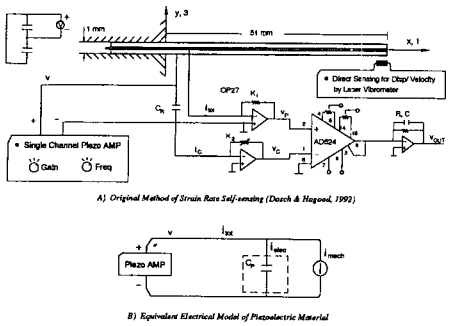

Fig. 1 Original method of strain rate self-sensing

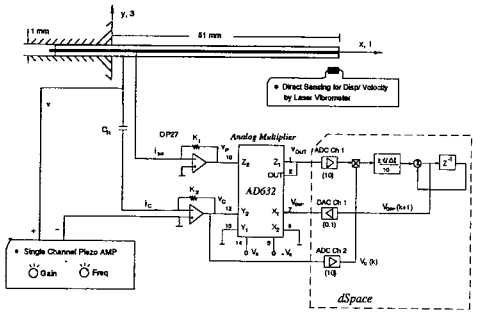

Fig. 2 Method of strain rate self-sensing using adaptive filter

(b) conceptually shows this phenomenon. It shows that only a portion (i_{mech}) of the total current (i_{tot}) is transformed into the useful mechanical energy. A self-sensing mechanism is a kind of estimator for this mechanical energy. Two methods of strain rate self-sensing are considered here. The circuit in Fig. 1(a) is the original method proposed by Anderson et al., and Dosch et al., in 1992. Figure 2 shows a circuit using a method developed by Clark (1995 ; 1998) employing an adaptive filter for a strain rate estimation.

2.1 The original method (Hagood and Dosch, 1992)

Figure 1(a) represents the original circuit for a strain rate sensing proposed by Hagood and Dosch in 1992. The one-dimensional constitutive equation for the piezoelectric beam is given by the following.

$$D_3=e_{31}\varepsilon_1+\in_{33}^{S}E_3$$
$$v=E_3h_P=\frac{h_P}{\in_{33}^{S}}(D_3-e_{31}\varepsilon_1) \quad (1)$$

The last relation of Eq. (1) can be rearranged further by introducing the electrode area, A.

$$v=\frac{h_P}{A\in_{33}^{S}}(AD_3-Ae_{31}\varepsilon_1)=\frac{1}{C_P}(q_{tot}-q_{mech}) \quad (2)$$

where, $q_{tot}=D_3A$

$q_{mech}=e_{31}A\varepsilon_1$

$C_P=\dfrac{\in_{33}^{S}A}{h_P}$

By differentiating of Eq. (2), the following current relation can be established.

$$i_{tot}=i_{elec}+i_{mech}=C_P\frac{dv}{dt}+i_{mech} \quad (3)$$

The Eq. (2) and (3) are the basic equations for a self-sensing mechanism. By measuring electrically either q_{mech} or i_{mech}, the mechanical strain, or its rate developed on a piezoelectric material can be estimated.

The electrical circuit of Fig. 1(a) is based on the Eq. (3). The reference capacitor, C_R is used to cancel the feed through current. The total supplied current (i_{tot}) and feed through current (i_{elec}) are converted into the voltage, v_P and v_C, and compared to each other using a high CMMR differential amplifier (Analog Device, AD524). Because of noise, a 1- st order LPF (Low Pass Filter) with the cutoff frequency of 5 kHz is applied at the final stage. The output voltage of AD524, which has a unity gain, is given by

$$v_S=v_P-v_C=(-K_1i_{tot})-\left(-K_2C_R\frac{dv}{dt}\right)$$
$$=-K_1i_{mech}+\frac{dv}{dt}(K_2C_R-K_1C_P) \quad (4)$$

The term inside the last parenthesis in Eq. (4) can be vanished by adjusting the variable resistor, K_2. After adjustment, the output voltage of the LPF is

$$v_{OUT}=\frac{K_1i_{mech}}{1+sRC}\cong K_1e_{31}A\frac{d\varepsilon_1}{dt} \quad (5)$$

If the value of C_P does not change during the operation of the piezoelectric material, the above method works perfectly. However, it is known that the value of a piezoelectric capacitance (C_P)

varies with the magnitude (q) and frequency (ω) of driving signal as well as with the operational temperature (T), and even with time (t).

$$C_P = f(q, \omega, T, t) \tag{6}$$

2.2 The method of adaptive filtering (Clark and Vipperman, 1995)

This method was developed by Clark and Vipperman in 1995. The original method of a strain self-sensing described in the above section works properly only under the stationary operating conditions for the piezoelectric material. If the operating conditions change, the recalibration of K_2 is necessary. Clark and Vipperman proposed a self-sensing mechanism using an adaptive filter, which obviates the troublesome manual tuning of K_2. Their concept is depicted in Fig. 2, which is mechanized using dSPACE™ DS1103 board. The AD632 IC in Fig. 2 is a high CMMR input analog multiplier which has the following transfer function.

$$\begin{aligned} v_{OUT} &= \frac{(X_1 - X_2)(Y_1 - Y_2)}{10} + Z_2 \\ &= v_P - \frac{v_C V_{DSP}}{10} \\ &= -K_1 i_{tot} + \frac{K_2}{10} i_C V_{DSP} \\ &= -K_1 \left\{ i_{mech} + \left(C_P - \frac{K_2}{10K_1} C_R V_{DSP} \right) \frac{dv}{dt} \right\} \end{aligned} \tag{7}$$

The term inside the small parenthesis in the above equation is similar to that of Eq. (4). The value of v_{OUT} in Eq. (7) is minimized automatically by adjusting V_{DSP} through a recursive adaptive filter instead of manual tuning as was done in Eq. (4).

The value of V_{DSP} is determined by minimizing the quadratic cost function of the following equation.

$$J(V_{DSP}) = v_{OUT}^2 \tag{8}$$

From Eq. (7) and (8), the cost function, $J(V_{DSP})$ is a quadratic form in V_{DSP}, which means that its global minimum uniquely exists. By using the steepest descent method, the direction of change of V_{DSP} is calculated as follows.

$$\frac{dV_{DSP}}{dt} = -\mu \nabla V_{DSP} J(V_{DSP}) \tag{9}$$

The term of $\nabla V_{DSP} J(V_{DSP})$ in Eq. (9) physically means the increasing direction of the cost function, $J(V_{DSP})$ for V_{DSP}. Therefore, the solution of this differential equation always gives the global minimum of $J(V_{DSP})$. And, the value of μ controls the convergence speed to the global minimum. The above differential equation can be approximated by the following difference equation of

$$\begin{aligned} \frac{dV_{DSP}}{dt} &\cong \frac{V_{DSP}(k+1) - V_{DSP}(k)}{\Delta t} \\ &= -2\mu v_{OUT}(k) \frac{\partial v_{OUT}}{\partial V_{DSP}} \end{aligned} \tag{10}$$

Therefore, $V_{DSP}(k)$ can be determined by the 1-st order recursive digital filter of

$$V_{DSP}(k+1) = V_{DSP}(k) + \frac{2\mu \Delta t}{10} v_{OUT}(k) v_C(k) \tag{11}$$

If $V_{DSP}(k)$ converges, then the capacitance of a piezoelectric material can be estimated by

$$C_P = \frac{K_2}{10K_1} C_R V_{DSP} \tag{12}$$

The difference equation of Eq. (11) is the main equation in the strain rate self-sensing using an adaptive filter algorithm. This filter dynamics are mechanized on the dSPACE™ 1103 DSP board as shown in Fig. 2.

3. Mathematical Model of a Cantilevered Piezoelectric Beam

The piezoelectric beam used in this paper is manufactured by the FUJI Ceramics (Model #: BM-ACT 03). A schematic diagram of the piezoelectric beam is shown in Fig. 3. It is composed of a central shim (Fe and Ni alloy) between two pieces of PZT materials with a coating material (RTV Silicone). The material properties are summarized in Table 1. From the assumption of an Euler-Bernoulli beam theory, only the bending stress in the cantilevered beam exists in the x-direction. Therefore, the displacement vector, U(X, t) for the beam motion can be simplified as a scalar function, $y(x, t)$, which can be approximated using the assumed mode method.

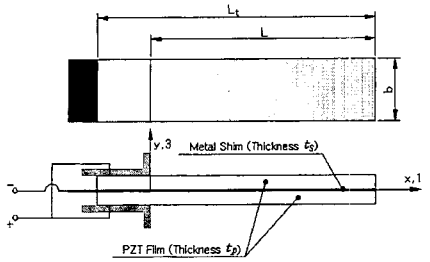

Fig. 3 Schematics of the cantilevered piezoelectric beam

$$U(X, t)=y(x, t)\cong\sum_{i=1}^{n}\phi_i(x)\,r_i(t) \tag{13}$$

where, $\phi_i(x)$: Admissible function satisfying geometric boundary condition

$r(t)=[r_1(t)\quad\cdots r_n(t)]^T$: Generalized coordinate vector

A mathematic model governing the motion of the piezoelectric cantilevered beam can be derived using Hamilton's principle and assumed mode method as follows.

$$\begin{aligned}&M_S\ddot{r}+C_D\dot{r}+K_Sr=\Theta v\\&q=\Theta^Tr+C_Pv\end{aligned} \tag{14}$$

where,

M_S : Mass matrix associated with center shim, piezoelectric and coating material $(n\times n)$

$$M_S=[m_{ij}]$$
$$=\left[(m_S+2m_P+2m_C)\int_0^L\phi_i(x)\,\phi_j(x)\,dx\right] \tag{15}$$
$$m_S=\rho_Sh_Sb$$
$$m_P=\rho_Ph_Pb$$
$$m_C=\rho_Ch_Cb$$

K_S : Stiffness matrix associated with center shim, piezoelectric and coating material $(n\times n)$

$$K_S=[k_{ij}]=\left[(E_SI_S+2E_PI_P+2E_CI_C)\int_0^L\phi_i''(x)\,\phi_j''(x)\,dx\right] \tag{16}$$
$$I_S=\frac{bh_S^3}{12}$$
$$I_P=\frac{b}{3}\left(h_P^3+\frac{3}{2}h_P^2h_S+\frac{3}{4}h_Ph_S^2\right)$$
$$I_C=\frac{b}{3}\left\{3\left(h_P+\frac{h_S}{2}\right)^2h_C+3\left(h_P+\frac{h_S}{2}\right)h_C^2+h_C^3\right\}$$

C_D : Damping matrix of the total structure $(n\times n)$

r : Generalized mechanical coordinate $(n\times1)$

Θ : Electromechanical coupling matrix $(n\times m)$

$$\Theta=\begin{pmatrix}-a\int_0^L\phi_1''(x)\,dx\\\vdots\\-a\int_0^L\phi_n''(x)\,dx\end{pmatrix} \tag{17}$$
$$a=\frac{e_{31}b}{h_P}\int_{hs/2}^{hs/2+hp}y\,dy=\frac{e_{31}b}{2}(h_S+h_P)$$
$$=\frac{d_{31}E_P^{11}b}{2}(h_S+h_P)$$

v : Generalized electrical coordinate (1×1)

q : Vector of applied electrode charge (1×1)

C_P : Diagonal matrix of piezoelectric capacitance (1×1)

$$C_P=2\frac{\in_{33}^S bL_t}{h_P} \tag{18}$$

It's difficult to analytically include the effect of damping on the beam motion. Therefore, the damping matrix C_D of Eq. (14) is developed through the coordinate transformation between the original and modal axis. Appropriate modal dampings are found from the comparison of analytic and experimental results.

To calculate the structural matrix of M_S, K_S, and Θ in Eq. (14), the following assumed mode, which is an admissible function satisfying the geometric boundary conditions of cantilevered beam, is used. For the approximation of $y(x, t)\cong\sum_{i=1}^{n}\phi_i(x)\,r_i(t)$, two admissible functions are used, i.e.

$$\phi_i(x)=\frac{x}{L}\sin\left(\frac{\pi x}{2L}i\right) \tag{19}$$
$$\phi_i(x)=\cosh\left(\frac{\pi x}{2L}i\right)-\cos\left(\frac{\pi x}{2L}i\right)-\frac{\sinh(\pi i/2)-\sin(\pi i/2)}{\cosh(\pi i/2)+\cos(\pi i/2)}\left(\sinh\left(\frac{\pi x}{2L}i\right)-\sin\left(\frac{\pi x}{2L}i\right)\right) \tag{20}$$

The admissible function of Eq. (20) is closer to the eigenfunction of a cantilevered beam problem than the one of Eq. (19). However, it turns out that this difference of admissible functions is not a factor, as there are no significant effects on the

Table 1 Characteristic data of the piezoelectric beam

Symbol	Description	Value	Dimension
L	Clamped length of piezoelectric beam	51	mm
L_t	Total length of piezoelectric beam	68	mm
h_P	Thickness of piezoelectric beam	0.45	mm
h_S	Thickness of elastic beam(Shim)	0.1	mm
h_C	Thickness of coating material(RTV silicone)	0.02	mm
b	Width of beam	10	mm
ρ_P	Density of piezoelectric material	7.75×10^3	kg/m^3
ρ_S	Density of shim material	8.2×10^3	kg/m^3
ρ_C	Density of coating material	1.16×10^3	kg/m^3
E_P^{11}	Young's modulus of piezoelectric material	5.9×10^{10}	N/m^2
E_S	Young's modulus of shim material	1.47×10^{11}	N/m^2
E_C	Young's modulus of coating material	6.2×10^8	N/m^2
d_{31}	Piezoelectric constant	-330×10^{-12}	m/V
$\in_{33}^T$	Relative permittivty of piezoelectric material	5500	F/m
C_P	Total capacitance of piezoelectric material	109.6	nF

resulting structural matrix of Eq. (14).

To evaluate the accuracy of the developed mathematical model, the experimental frequency response is found. The experimental setup for this work is exactly the same as that depicted in Fig. 2 except that the frequency response analyzer (ONO SOKKI, CF350 Dual Channel FFT Analyzer) drives the cantilevered piezoelectric beam. The end point displacement of the piezoelectric beam is picked up by the laser displacement sensor (Keyence LD-2500 (10 mV/μm sensitivity)). The analytical and experimental frequency response of the beam end point are plotted together in Fig. 4. The modal damping of 0.01 is used for all the modal frequencies. The dashed line is the analytical result and the other is for the experimental result. The analytical frequency response is shifted up 4.4 dB to match DC gain with the experimental results in this figure. The analytical frequency response is almost the same as that of experimental one except that it is shifted to the right on the frequency axis. The comparison of modal frequencies is shown on Table 2. Approximately, 5% relative error between the analytic and experimental modal frequency is resulted. The analytic and experimental step responses of the beam end point for 10 Volt driving are shown in Fig. 5. The lower one is the analytic response, which has the DC gain of about 0.675 (−3.4 dB) times less than that of the experimental one.

Table 2 Comparison of analytic and experimental modal frequencies

Modal Frequency	Experiment (Hz)	Analysis (Hz)	% Error
1 - st mode	160	168.5	5.31
2 - nd mode	1025	1059	3.31
3 - rd mode	2850	2988	4.84
4 - th mode	5625	5962	5.99

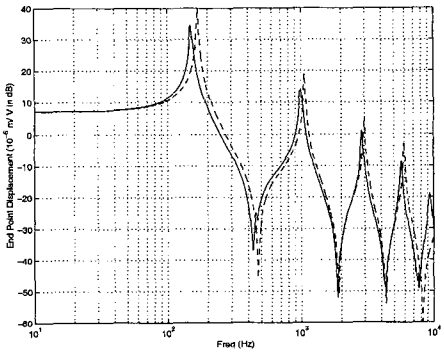

Fig. 4 The frequency response of beam end point displacement (analytical and experimental)

4. Experiments on Strain Rate Self-Sensing Using Adaptive Filter

The resistor value of K_2 in Fig. 2 is chosen as 2 $k\Omega$ in order for V_{DSP} to be within linear opera-

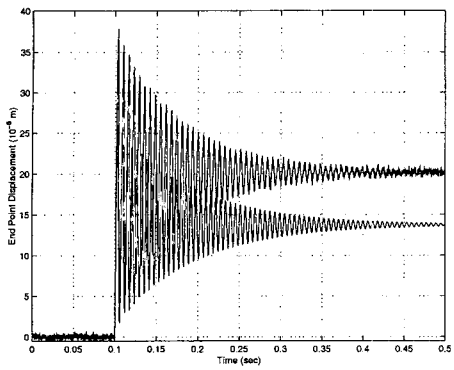

Fig. 5 The analytical and experimental step responses for 10 V driving signal

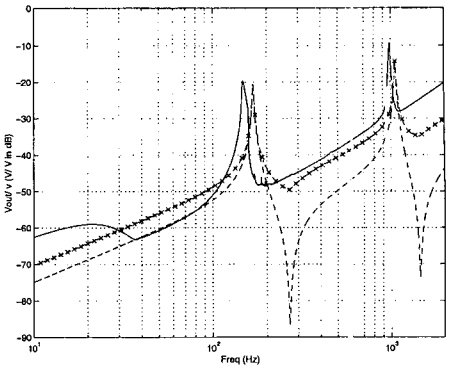

Fig. 6 The frequency response of v_{OUT} from adaptive filter

tion range. The use of smaller value of K_2 like 1 $k\Omega$ makes the magnitude of V_{DSP} to be at around 10 Volt due to the relation of Eq. (7), which is near the saturation range of the dSPACE™ 1103 DSP board. It turns out the convergence of V_{DSP} is not guaranteed for some driving frequencies in case of using 1 $k\Omega$ for K_2. The experimental frequency response of v_{OUT} for the excitation signal of v is shown as the solid line in Fig. 6 with the analytic result, which is the dashed line. The sampling time of the digital adaptive filter is 100 μs, and the convergence factor (μ) is set as a 400 in this experiment. There are two points that should be mentioned in the comparison with two responses. One is the DC level difference. The other, which is much more critical, is that the experimental frequency response does not show the effects of zero. The main reason for these is considered due to the hysteresis phenomenon of the piezoelectric materials. Because the piezoelectric materials are ferroelectric, they fundamentally exhibit hysteresis behavior in their response to an applied electric field (Ping and Jouaneh, 1996). The hysteresis loop is a consequence of the effects of domain switching due to the action of the external applied cyclic electric field. Since each domain is a composition of several parallel dipoles, the effective number of dipoles aligned in the direction of the electric field will be altered as domains switch under the action of an external electric field. This domain switching does not occur instantaneously and it is this delay response which gives rise to the hysteresis loop. Therefore, the current flow (i_{tot}) through the piezoelectric material has the phase delay compared to the current flow (i_c) through the reference capacitance in Fig. 2.

In order to see the effect of the phase delay from a piezoelectric material on the performance of a strain rate self-sensing circuit, it's assumed that $i_{mech}=0$. This assumption is almost true for the excitation at any zero frequencies. Then, for the excitation input of $v=v_0 \sin \omega t$,

$$\begin{aligned} v_{out} &= v_p - \frac{v_c v_{DSP}}{10} = -K_1 C_p \left(\frac{dv}{dt}\right)_P \\ &\quad - \frac{K_2}{10} C_r V_{DSP} \left(\frac{dv}{dt}\right)_C \\ &= -v_0 \omega K_1 C_p \cos(\omega t - \phi) \\ &\quad + \frac{v_0 \omega K_2 C_r}{10} V_{DSP} \cos \omega t \\ &\cong -\frac{v_0 \omega K_2 C_r \phi}{10} V_{DSP} \sin \omega t \\ &= -v_0 \omega K_1 C_p \phi \sin \omega t \end{aligned} \tag{21}$$

In the above derivation, the perfect functioning of the adaptive filter is assumed, i.e.

$$V_{DSP} = \frac{10 C_p K_1}{C_r K_2} \tag{22}$$

The validity of the above analysis can be evaluated by the investigation of the experimental frequency response in Fig. 6. The analytical frequency response of v_{OUT}, which is calculated based on the assumption of the phase delay of 1°, is shown as the dash-dot line with 'x' mark in this figure. The disappearance of zero effects due to the phase delay in the frequency response can be noticed. If the frequency information can be extracted from the driving signal in real-time, the

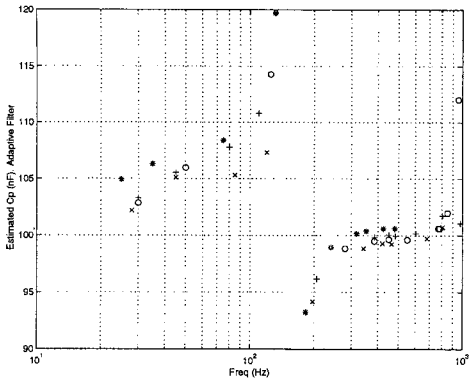

Fig. 7 The estimated capacitance of piezoelectric material

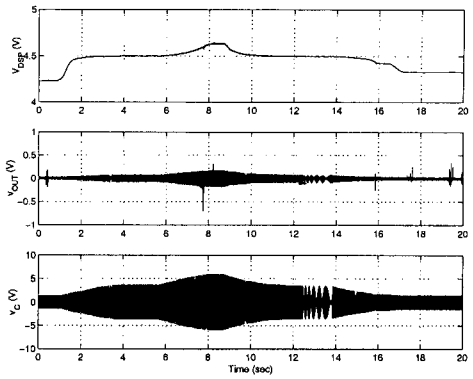

Fig. 8 The variation of V_{DSP}, v_{OUT}, and v_C for sweeping sine input (μ= 400)

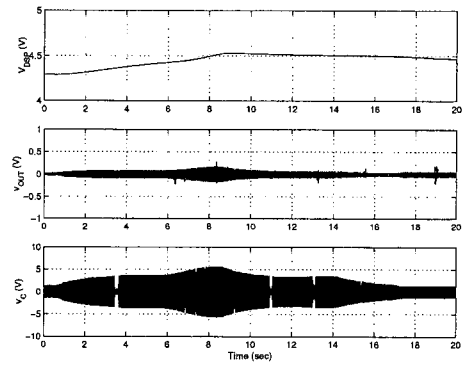

Fig. 9 The variation of V_{DSP}, v_{OUT}, and v_C for sweeping sine input (μ=2)

phase delay effects can be cancelled out from the adaptive filtering.

The capacitance of the piezoelectric material is estimated based on the experimental data on the self-sensing circuit using adaptive filtering. The manufacturer (FUJI Ceramics) supplied data of the piezoelectric capacitance has a value of 109.6 nF. Eq. (12) can be used to estimate the capacitance of piezoelectric material. The experimental results are shown in Fig. 7. The points marked as '*', '+', 'o', and 'x' in this figure show the values of the estimated capacitance at each excitation frequency for the driving signal magnitudes of 20.5 V_{PP}, 12.5 V_{PP}, 8.75 V_{PP}, and 5.5 V_{PP}, respectively. Based on these data, the estimated capacitance of the piezoelectric material seems to be affected by the cantilever beam motion dynamics.

The effect of convergence factor, μ in Eq. (9) can be noticed in Fig. 8 and Fig. 9. The experimental data for V_{DSP}, v_{OUT}, and v_C are shown in Fig. 8 for the value of μ=400, and in Fig. 9 for that of μ=2. These data are obtained by varying the excitation signal frequency while keeping its magnitude constant at 10 V_{PP}. The signal frequency is varied continuously from 200 Hz to 800 Hz, and back to the 200 Hz using a function generator. The magnitude of v_{OUT} is much smaller than that of v_C, indicating that the adaptive filter is functioning in the strain rate self-sensing circuit. The slow convergence of V_{DSP} in Fig. 9 is because of using the small value of convergence factor, μ. The peak-to-peak value of v_{OUT} at the final stage (around 20 seconds in Fig. 9) becomes larger than the initial value by the factor of two due to the slow convergence of V_{DSP}. The peak-to-peak values of v_{OUT} at the final stage for μ=400, however, are almost same order of magnitude at the initial and final stage, as can be seen in Fig. 8.

The several observations can be made based on the analysis of the experimental results. The strain rate self-sensing mechanism using an adaptive filtering (Vipperman, 1995 and Clark, 1998), which is applied to the problem of a cantilevered piezoelectric beam, does not work properly in the points that the zero frequency dynamics of the beam motion are not possible to identify experimentally and the estimated capacitance of the piezoelectric material (or V_{DSP} at the steady state, by referring Eq. (12)) changes its value according to the variation of the beam dynamics.

The main reason of disappearing zero dynamics is considered as the phase delay in the piezoelectric material. And, the variation of the estimated piezoelectric capacitance with the beam motion is supposed to be the byproduct of using an adaptive filtering structure. This can be explained by the further analysis on Eq. (7) - Eq. (9).

$$\frac{dV_{DSP}}{dt} = -\mu \nabla V_{DSP} J(V_{DSP}) = 2\mu \frac{v_c v_{out}}{10} = \frac{2\mu}{10} K_1 K_2 C_r \left(\frac{dv}{dt}\right) \left\{\left(C_p - \frac{K_2}{10K_1} C_r V_{DSP}\right)\left(\frac{dv}{dt}\right) + i_{mech}\right\} \quad (23)$$

As can be seen in the above equation, V_{DSP} at the steady state is dependant on the magnitude of i_{mech}. Therefore, the magnitude of V_{DSP} would have the relatively larger value at the pole frequencies of the cantilevered beam dynamics than that at the other frequencies. This reasoning is supported by the experimental results of Fig. 8, in which the large values of the piezoelectric capacitance (or V_{DSP}) are noticed at the modal frequencies of 160 Hz and 1025 Hz.

5. Conclusion

The problem of the strain rate self-sensing is considered both analytically and experimentally for a cantilevered PZT beam. The self-sensing structure is implemented using a hybrid adaptive filter based on the steepest descent algorithm. A mathematical model is derived by the application of Hamilton's principle to the cantilevered piezoelectric beam. The major discrepancies between the experimental and analytical results of the strain rate self-sensing are the magnitude differences near the zero frequencies of the cantilevered beam dynamics. It is believed that these are due to the phase delay effect of the piezoelectric material. It turns out also that the estimated capacitance of the piezoelectric material is affected by the cantilever beam motion dynamics. This is considered to be the natural consequence in using an adaptive filtering for a strain rate self-sensing. The future research areas are focused on finding the new and systematic self -sensing mechanism to estimate the strain rate variation of the piezoelectric structure and the estimator design of the beam end point displac -ment from the strain rate self-sensing information.

Acknowledgements

This work was supported by grant No. 2001-1-30400-014-1 from the Basic Research Program of the Korean Science & Engineering Foun-dation.

References

Anderson, E., Hagood, N. Goodliffe, E., 1992, "Self-Sensing Piezoelectric Actuation: Analysis and Application to Collocated Structures," *33-rd AIAA/ ASME/ASCE/AHS/ASC Structure, Structural Dynamics, and Materials conf.*, AIAA -92-2465, pp. 2141~2155.

Clark, R. Fuller, C., 1992, "Experiments on Active Control of Structurally Radiated Sound Using Multiple Piezoceramic Actuators," *J. of Acoustic Society of America*, Vol. 91, No. 6, pp. 3313~3320.

Clark, R., Saunders, W. and Gibbs, G., 1998, *Adaptive Structures Dynamics and Control*, John Wiley & Sons.

Cole, D. and Clark, R., 1994, "Adaptive Compensation of Piezoelectric Sensoriactuators," *Journal of Intelligent Material Systems and Structures*, Vol. 5, pp. 665~672.

Crawley, E. and Luis, J., 1987, "Use of Piezoelectric Actuators as Elements of Intelligent Structures," *AIAA Journal*, Vol. 25, No. 10, pp. 1373~1385.

Dimitriadis, E. Fuller, C. and Rogers, C., 1991 "Piezoelectric Actuators for Distributed Vibration Excitation of Thin Plates," *Trans. of ASME, J. of Vibration and Acoustics*, Vol. 113, pp. 100 ~107.

Doebelin, E., 1990, *Measurement Systems Application and Design*, McGraw-Hill.

Dosch, J., and Inman, D., Garcia, E., 1992, "A Self-Sensing Piezoelectric Actuator for Collocated Control," *J. of Intelligent Material Systems and Structures*, Vol. 3, pp. 166~183.

Evans, R., Griesbach, J. Messner, W., 1999,

"Piezoelectric Microactuator for Dual Stage Control," *IEEE Trans. on Magnetics*, Vol. 35, pp. 977~982.

Fannin, C. and Saunders, W., 1997, "Analog Adaptive Piezoelectric Sensoriactuator Design," *Proceedings of the AIAA SDM Conference*.

Ishihara, H. and Arai, F., 1996, "Micro Mechatronics and Micro Actuators," *IEEE/ ASME Transactions on Mechatronics*, Vol. 1, No. 1, pp. 68~79.

Janocha, H., Jenderitza, D. and Scheer, P., 1996, "Smart Actuators with Piezoelectric Material," *3-rd ICIM/ ECSSM '96*, pp. 603~609.

Johns, L., Garcia, E. Waites, H., 1994, "Self -Sensing Control as Applied to PZT Stack Actuator Used as a Micropositioner," *J. of SPIE*, Vol. 2190, pp. 228~237.

Ko, B., 1996, "Active Noise Control Using Sensory Actuator," *Transactions of KSME Series A*, Vol. 20, No. 5, pp. 1573~1581.

Oh, J., Park, S., Hong, J. and Shin, J., 1998, "Active Vibration Control of Flexible Cantilever Beam Using Piezo Actuator and Filtered-X LMS Algorithm," *KSME International Journal*, Vol. 12, No. 4, pp. 665~671.

Okugawa, M. Sasaki, M., 1997, "Robust Motion Control of a Flexible Micro-Actuator Using LQG/ LTR Design Method," *Transactions of JSME Series C*, Vol. 63, No. 616, pp. 194~199.

Ge, Ping and Jouaneh, Musa 1996, "Tracking Control of a Piezoceramic Actuator," *IEEE Transactions on Control System Technology*, Vol. 4. , No. 3, pp. 209~216.

Vipperman, J. and Clark, R., 1995, "Hybrid Analog and Digital Adaptive Compensation of Piezoelectric Sensoriactuator," *AIAA/ ASME/ Adaptive Structures Forum*, pp. 2854~2859.